

# A Density Functional Study of Open-Shell Cyclopentadienyl–Molybdenum(II) Complexes. A Comparison of Stabilizing Factors: Spin-Pairing, Mo–X $\pi$ Bonding, and Release of Steric Pressure

Ivo Cacelli,<sup>†</sup> Rinaldo Poli,<sup>\*,‡</sup> Elsje Alessandra Quadrelli,<sup>§</sup> Antonio Rizzo,<sup>§</sup> and Kevin M. Smith<sup>‡</sup>

Scuola Normale Superiore, Piazza dei Cavalieri 7, I-56126 Pisa, Italy, Laboratoire de Synthèse et d'Electrosynthèse Organométalliques, Faculté des Sciences "Gabriel", Université de Bourgogne, 6 Boulevard Gabriel, F-21000 Dijon, France, and Istituto di Chimica Quantistica ed Energetica Molecolare del Consiglio Nazionale delle Ricerche, Via Risorgimento 35, I-56126 Pisa, Italy

Received July 23, 1999

The dissociation of  $\text{PH}_3$  from the 18-electron system  $\text{CpMoX}(\text{PH}_3)_3$  to afford the corresponding 16-electron  $\text{CpMoX}(\text{PH}_3)_2$  fragment has been investigated theoretically by density functional theory for  $\text{X} = \text{H}, \text{CH}_3, \text{F}, \text{Cl}, \text{Br}, \text{I}, \text{OH},$  and  $\text{PH}_2$ . The product is found to prefer a triplet spin state for all X ligands except  $\text{PH}_2$ , the singlet–triplet gap varying between 1.7 kcal/mol for OH to 8.7 kcal/mol for F. The Mo– $\text{PH}_3$  bond dissociation energy to the 16-electron ground state varies dramatically across the series, from 4.5 kcal/mol for OH to 23.5 kcal/mol for H, and correlates with experimental observations on trisubstituted phosphine derivatives. Geometry-optimized spin doublet  $\text{CpMo}(\text{PH}_3)_3$ , on the other hand, has a Mo– $\text{PH}_3$  bond dissociation energy of 24.3 kcal/mol. The modulation of the Mo– $\text{PH}_3$  bond dissociation energy by the introduction of X is analyzed in terms of three effects that stabilize the 16-electron product relative to the 18-electron starting complex: (i) adoption of the higher (triplet) spin state by release of pairing energy; (ii) Mo–X  $\pi$  interactions; (iii) release of steric pressure. A computational model for the approximate separation and evaluation of these three stabilizing effects is presented. According to the results of these calculations, the relative importance of the three effects depends on various factors related to the nature of X. For double-sided  $\pi$ -donor X ligands, the larger triplet–singlet gap is provided by the more electronegative atoms ( $\text{F} > \text{Cl} > \text{Br} > \text{I}$ ), whereas single-sided  $\pi$  donors favor the singlet state. The  $\pi$ -stabilization ability goes in the order  $\text{PH}_2 > \text{OH} > \text{F} > \text{other halogens} > \text{H}$ . Finally, the major steric interaction appears to be associated with the presence of inactive lone pairs and by their orientation/proximity to the  $\text{PH}_3$  ligands ( $\text{Cl}, \text{Br} > \text{I}, \text{OH} > \text{F}, \text{PH}_2, \text{H}, \text{CH}_3$ ). The 16-electron methyl system establishes a marked  $\alpha$ -agostic interaction in the singlet state, which nevertheless remains unfavored relative to an undistorted triplet configuration.

## Introduction

The chemistry of organometallic compounds is dominated by the 18-electron rule and by diamagnetism.<sup>1</sup> This is the direct consequence of three factors: the high bond covalency in this realm of chemistry, the ability of the ligands to establish  $\pi$  back-bonding interactions with the central metallic element, and the relatively low electron–electron repulsion enabling the establishment of spin-paired configurations. Electronically unsaturated (open-shell) configurations are, however, frequently associated with reaction intermediates (this being the basis of Tolman's "16 and 18-electron rule"),<sup>2</sup> and can lead to the isolation of stable compounds under favorable circumstances. A clear understanding of the factors at work in the stabilization of open-shell structures relative to saturated counterparts is therefore fundamental for the rationalization of reaction rates and catalytic activity.

Complexes having a 16-electron configuration may be accessed from closed-shell precursors in several ways, e.g.

ligand dissociation, reductive elimination, migratory insertion, and so on. Four mechanisms may be distinguished for their energetic stabilization relative to the saturated precursor: (i) release of steric pressure associated with the decrease of inter-ligand repulsive van der Waals interactions<sup>3</sup>; (ii) intervention of ligand lone pairs ( $\pi$  donation)<sup>4,5</sup>; (iii) release of pairing energy (this playing a role only when the open-shell and saturated species have different spin states)<sup>6</sup>; (iv) interactions, including agostic ones, with other donor molecules (e.g. the solvent) or groups (e.g. dangling donor functions from ligands). The fourth mechanism effectively consists of the temporary saturation of the open coordination site (replacement of a ligand with a more labile one), rather than the relative stabilization of an unsaturated structure. It is responsible, for instance, for the acceleration of many reactions involving a rate-determining dissociative step when these are carried out in donor solvents. This article focuses only on the analysis of the first three effects, although the intervention of intramolecular  $\alpha$ -agostic interactions will be highlighted in a particular case.

The relative importance of each of these effects cannot be determined or estimated easily. We will be concerned here with

<sup>†</sup> Scuola Normale Superiore.

<sup>‡</sup> Université de Bourgogne.

<sup>§</sup> Istituto di Chimica Quantistica ed Energetica Molecolare del Consiglio Nazionale delle Ricerche.

(1) Collman, J. P.; Hegedus, L. S.; Norton, J. R.; Finke, R. G. *Principles and Applications of Organotransition Metal Chemistry*; University Science Books: Mill Valley, CA, 1987.

(2) Tolman, C. A. *Chem. Soc. Rev.* **1972**, 1, 337–353.

(3) Tolman, C. A. *Chem. Rev.* **1977**, 77, 313–348.

(4) Caulton, K. G. *New J. Chem.* **1994**, 18, 25–41.

(5) Ashby, M. T. *Comments Inorg. Chem.* **1990**, 10, 297–313.

(6) Poli, R. *Chem. Rev.* **1996**, 96, 2135–2204.

the formation of half-sandwich 16-electron Mo(II) complexes by ligand dissociation from 18-electron precursors, but the arguments may be extrapolated to any other reaction generating a 16-electron from an 18-electron compound or any ( $n-2$ )-electron from an  $n$ -electron compound. We will use CpMoX(PH<sub>3</sub>)<sub>2</sub> as a model for the bis-PMe<sub>3</sub> complexes previously used by us in several studies.<sup>7–11</sup> The relevance of a sterics-related stabilization is indicated experimentally by the equilibrium between Cp\*MoCl(PMe<sub>3</sub>)<sub>3</sub> and the mixture of Cp\*MoCl(PMe<sub>3</sub>)<sub>2</sub> and PMe<sub>3</sub> at room temperature, or between CpMoCl(PMe<sub>2</sub>Ph)<sub>3</sub> and the mixture of CpMoCl(PMe<sub>2</sub>Ph)<sub>2</sub> and PMe<sub>2</sub>Ph upon warming, whereas no phosphine loss was observed for CpMoCl(PMe<sub>3</sub>)<sub>3</sub> under the same conditions.<sup>8</sup> The absence of any CpMo(OH)(PMe<sub>3</sub>)<sub>3</sub> in equilibrium with a mixture of CpMo(OH)(PMe<sub>3</sub>)<sub>2</sub> and PMe<sub>3</sub>,<sup>10,11</sup> on the other hand, demonstrates the intervention of additional stabilizing factors (OH occupies less space than Cl). Both Cl and OH have lone pairs and are thus capable of providing  $\pi$  stabilization. It is generally believed that a hydroxo ligand is a stronger  $\pi$  donor than the halogens but quantitative assessment, to our knowledge, are not available. On the other hand, because the stable 16-electron systems Cp\*MoCl(PMe<sub>3</sub>)<sub>2</sub> and CpMo(OH)(PMe<sub>3</sub>)<sub>2</sub> exhibit a spin triplet ground state, a stabilizing factor associated with the release of pairing energy must also play a role.

The quantitative evaluation of  $\pi$ -bond strengths is a difficult exercise.<sup>4</sup> It requires the separation of  $\sigma$ - and  $\pi$ -bonding components, which is experimentally impossible and theoretically nonrigorous.<sup>12–14</sup> From the experimental point of view, qualitative evaluations of trends in M–X  $\pi$ -bond strengths, these relating in most cases to bonds between a metal and the halogens, have been deduced from the analysis of NMR chemical shifts,<sup>15</sup> EPR  $g$  values,<sup>16</sup> IR carbonyl stretching frequencies,<sup>17,18</sup> electrochemical data,<sup>19,20</sup> UV–visible spectra,<sup>21,22</sup> valence photoelectron spectra,<sup>23</sup> X-ray crystal structures,<sup>24,25</sup> and rates of chemical and fluxional processes or even the simple observation

that certain reactions take place whereas others do not.<sup>26–29</sup> The use of such a wide array of techniques, each necessitating a different set of assumptions and approximations, has led to controversy. For instance, no universal agreement has been achieved about whether a lighter donor atom is a weaker or a stronger  $\pi$  donor than a heavier congener (e.g. Cl vs I or SR vs TeR); the relative donor power may well depend on the nature of the metal and on the chemical environment. From the point of view of theory, different localization and partition schemes have been used,<sup>14,30–40</sup> but, to the best of our knowledge, these have not been applied to characterize the nature of the metal-to-ligand bonding in transition metal complexes of the kind studied here.

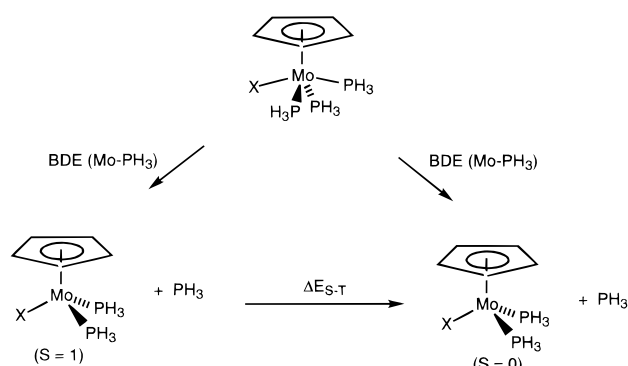
In a recent article,<sup>11</sup> we have presented a new computational model that has allowed us, within certain approximations, to differentiate the contributions of interligand repulsion,  $\pi$  donation, and electron pairing to the relative stabilization of the CpMoX(PH<sub>3</sub>)<sub>2</sub> model systems. We have now refined this model and extended it to a wider range of X ligands. The results reported herein allow, among other things, a rough quantitative estimation of the Mo–X  $\pi$ -bond strength.

### Computational Details

All electronic structure and geometry optimization calculations were performed using Gaussian-94<sup>41</sup> on an SGI Origin 200 workstation at the Université de Bourgogne and on both an Alpha Digital and an SGI Indigo 2 in Pisa. The three-parameter form of the Becke, Lee, Yang, and Parr functional (B3LYP),<sup>42</sup> was used. The LanL2DZ basis set includes both Dunning and Hay's D95 sets for H, C, O, and F<sup>43</sup> and the relativistic Electron Core Potential (ECP) sets of Hay and Wadt for the 10 inner electrons of Cl and P, the 18 inner electrons of Br, and the 28 inner electrons of Mo and I.<sup>44–46</sup> Unless otherwise

- (7) Abugideiri, F.; Keogh, D. W.; Poli, R. *J. Chem. Soc., Chem. Commun.* **1994**, 2317–2318.
- (8) Abugideiri, F.; Fetting, J. C.; Keogh, D. W.; Poli, R. *Organometallics* **1996**, *15*, 4407–4416.
- (9) Keogh, D. W.; Poli, R. *J. Am. Chem. Soc.* **1997**, *119*, 2516–2523.
- (10) Fetting, J. C.; Kraatz, H.-B.; Poli, R.; Quadrelli, E. A. *Chem. Commun.* **1997**, 889–890.
- (11) Poli, R.; Quadrelli, E. A. *New J. Chem.* **1998**, *22*, 435–450.
- (12) Chisholm, M. H.; Clark, D. L. *Comments Inorg. Chem.* **1987**, *6*, 23–40.
- (13) Kapp, J.; Schade, C.; El-Nahasa, A. M.; von Ragué Scheleyer, P. *Angew. Chem., Int. Ed. Engl.* **1996**, *35*, 2236–2237.
- (14) González-Blanco, O.; Brachadell, V.; Monteyne, K.; Ziegler, T. *Inorg. Chem.* **1998**, *37*, 1744–1748.
- (15) Gross, Z.; Mohammed, A.; Barzilay, C. M. *Chem. Commun.* **1998**, 1105–1106.
- (16) Lukens, W. W.; Smith, M. R., III.; Andersen, R. A. *J. Am. Chem. Soc.* **1996**, *118*, 1719–1728.
- (17) Poulton, J. T.; Folting, K.; Streib, W. E.; Caulton, K. G. *Inorg. Chem.* **1992**, *31*, 3190–3191.
- (18) Poulton, J. T.; Sigalas, M. P.; Folting, K.; Streib, W. E.; Eisenstein, O.; Caulton, K. G. *Inorg. Chem.* **1994**, *33*, 1476–1485.
- (19) Hogarth, G.; Konidaris, P. C.; Saunders, G. C. *J. Organomet. Chem.* **1991**, *406*, 153–157.
- (20) Tilset, M.; Hamon, J.-R.; Hamon, P. *J. Chem. Soc., Chem. Commun.* **1998**, 765–766.
- (21) Lever, A. B. P. *Inorganic Electronic Spectroscopy*, 2nd ed.; Elsevier: New York, 1984.
- (22) Bendix, J.; Bøgevig, A. *Inorg. Chem.* **1998**, *37*, 5992–6001.
- (23) Lichtenberger, D. L.; Rai-Chaudhuri, A.; Seidel, M. J.; Gladysz, J. A.; Agbossou, S. K.; Igau, A.; Winter, C. H. *Organometallics* **1991**, *10*, 1355–1364.
- (24) Chisholm, M. H.; Hammond, C. E.; Huffman, J. C. *Polyhedron* **1989**, *8*, 1419–1423.
- (25) Johnson, T. J.; Folting, K.; Streib, W. E.; Martin, J. D.; Huffman, J. C.; Jackson, S. A.; Eisenstein, O.; Caulton, K. G. *Inorg. Chem.* **1995**, *34*, 4, 488–499.
- (26) Atwood, J. D.; Brown, T. L. *J. Am. Chem. Soc.* **1976**, *98*, 3160–3166.
- (27) Bryndza, H. E.; Domaille, P. J.; Paciello, R. A.; Bercaw, J. E. *Organometallics* **1989**, *8*, 379–385.
- (28) Buhro, W. E.; Chisholm, M. H.; Folting, K.; Huffman, J. C.; Martin, J. D.; Streib, W. E. *J. Am. Chem. Soc.* **1992**, *114*, 557–570.
- (29) Cooper, A. C.; Bollinger, J. C.; Caulton, K. G. *New J. Chem.* **1998**, 473–480.
- (30) Edmiston, C.; Ruedenberg, K. *Rev. Mod. Phys.* **1963**, *35*, 457.
- (31) Edmiston, C.; Ruedenberg, K. *J. Chem. Phys.* **1965**, *43*, S97–S116.
- (32) Edmiston, C.; Ruedenberg, K. In *Quantum Theory of Atoms, Molecules and Solid State. A Tribute to John C. Slater*; P.-O. Löwdin, Ed.; Academic Press: New York, 1966; pp 263–280.
- (33) Pipek, J.; Mezey, P. G. *J. Chem. Phys.* **1989**, *90*, 4916–4926.
- (34) Uneyama, H.; Morokuma, K. *J. Am. Chem. Soc.* **1976**, *98*, 7208–7220.
- (35) Kitaura, K.; Morokuma, K. *Int. J. Quantum Chem.* **1976**, *10*, 325–340.
- (36) Bagus, P. S.; Hermann, K.; Bauschlicher, C. W., Jr. *J. Chem. Phys.* **1984**, *80*, 4378–4386.
- (37) Bagus, P. S.; Hermann, K.; Bauschlicher, C. W., Jr. *J. Chem. Phys.* **1984**, *81*, 1966–1974.
- (38) Bauschlicher, C. W., Jr. *Chem. Phys.* **1986**, *106*, 391–398.
- (39) Ziegler, T.; Rauk, A. *Theor. Chim. Acta* **1977**, *46*, 1–10.
- (40) Ziegler, T.; Rauk, A. *Inorg. Chem.* **1979**, *18*, 1558–1565.
- (41) Frisch, M. J.; Trucks, G. W.; Schlegel, H. B.; Gill, P. M. W.; Johnson, B. G.; Robb, M. A.; Cheeseman, J. R.; Keith, T. A.; Petersson, G. A.; Montgomery, J. A.; Raghavachari, K.; Al-Laham, M. A.; Zakrzewski, V. G.; Ortiz, J. V.; Foresman, J. B.; Cioslowski, J.; Stefanov, B. B.; Nanayakkara, A.; Challacombe, M.; Peng, C. Y.; Ayala, P. Y.; Chen, W.; Wong, M. W.; Andres, J. L.; Replogle, E. S.; Gomperts, R.; Martin, R. L.; Fox, D. J.; Binkley, J. S.; Defrees, D. J.; Baker, J.; Stewart, J. P.; Head-Gordon, M.; Gonzales, C.; Pople, J. A. *Gaussian 94*, Revision E.1; Gaussian Inc.: Pittsburgh, PA, 1995.
- (42) Becke, A. D. *J. Chem. Phys.* **1993**, *98*, 5648–5652.
- (43) Dunning, T. H., Jr.; Hay, P. J. In *Modern Theoretical Chemistry*; H. F. Schaefer, III, Ed.; Plenum Press: New York, 1976; pp 1–28.
- (44) Hay, P. J.; Wadt, W. R. *J. Chem. Phys.* **1985**, *82*, 270–283.
- (45) Wadt, W. R.; Hay, P. J. *J. Chem. Phys.* **1985**, *82*, 284–298.

Scheme 1



stated, calculations were performed without spatial symmetry constraints. The energies reported for the open-shell systems correspond to unrestricted (UB3LYP) calculations. In our<sup>47–49</sup> and other's<sup>50–52</sup> experience, this computational method correctly reproduces the experimentally observed spin state for open-shell systems. For open-shell systems the mean value of the spin over the electronic density in unrestricted calculations does not reproduce exactly the assigned spin multiplicity. In all our cases, however, it was considered to be suitable to identify unambiguously the spin state. Mean values of  $\langle S^2 \rangle$  were in the narrow 2.012–2.015 range for triplets.

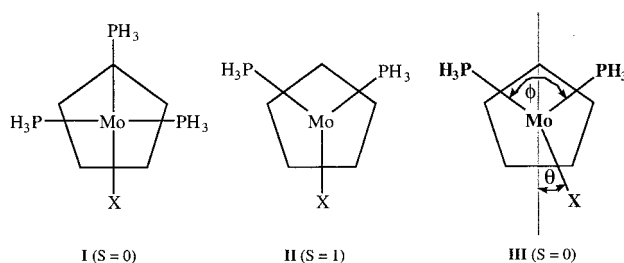
## Results and Discussion

**a. Geometries and Mo–PH<sub>3</sub> Bond Dissociation Energies. Singlet vs Triplet CpMoX(PH<sub>3</sub>)<sub>2</sub>.** The considerations presented in this article are based on the energetics of the dissociation of one phosphine ligand on the model system CpMoX(PH<sub>3</sub>)<sub>3</sub> (X = H, CH<sub>3</sub>, F, Cl, Br, I, OH, PH<sub>2</sub>) (see Scheme 1). The Mo–PH<sub>3</sub> bond dissociation energy (BDE) relates the 18-electron CpMoX(PH<sub>3</sub>)<sub>3</sub> complex and the combination of 16-electron CpMoX(PH<sub>3</sub>)<sub>2</sub> and free PH<sub>3</sub>, all geometry optimized. The BDEs relative to both singlet and triplet 16-electron products are presented in Table 1. Although the 18-electron complex adopts a singlet ground state, the 16-electron complex has the lowest lying triplet configuration in all cases, except for the phosphido derivative.

We have calculated the basis set superposition error (BSSE)<sup>53</sup> for the fluoride system using the counterpoise technique,<sup>54</sup> and found a decrease of 2.9 kcal/mol for the Mo–PH<sub>3</sub> BDE. Because the BSSE depends largely on the bond distance and because the Mo–PH<sub>3</sub> bond length is essentially independent of X, we presume that all BDEs reported in Table 1 should be scaled down by the same amount. A reduction of all BDEs may in fact lead to a better agreement with available experimental data, as the lowest BDE for the OH system may be compared with the stability of triplet CpMo(OH)(PMe<sub>3</sub>)<sub>2</sub> in the presence of excess PMe<sub>3</sub>.<sup>10,11</sup>

The geometry optimized 18-electron and the triplet 16-electron systems correspond to essentially C<sub>s</sub>-symmetric structures which can be described, respectively, as four- and three-

legged piano stools (see **I** and **II**). The singlet 16-electron systems, on the other hand, have optimized geometries exhibiting a certain degree of asymmetry. Two different minima were located for each X, the lowest one corresponding in all cases except for X = H to a C<sub>1</sub> geometry where the ligand X has more or less deviated from the P–Mo–P bisector plane, as illustrated schematically in **III**. The second minimum (lowest for X = H) is an essentially C<sub>s</sub>-symmetric structure where the P–Mo–P angle has more or less increased relative to the triplet **II**. The distortion from a regular (pseudo-octahedral) structure as found in the triplet can be assessed by two dihedral angles. The angle  $\theta$  is the angle formed by the CNT–Mo–X plane and the plane passing through CNT, Mo, and the bisector of the two Mo–PH<sub>3</sub> bonds, whereas the angle  $\phi$  is the dihedral P–Mo–CNT–P angle (CNT is the Cp ring centroid), see **III**. The values of the angles  $\theta$  and  $\phi$  for the lowest energy optimized CpMoX(PH<sub>3</sub>)<sub>2</sub> ( $n = 2, 3$ ) are reported in Table 2 together with the Mo–X distances. In most cases, the Mo–CNT and Mo–PH<sub>3</sub> distances for **I** have intermediate values between those of **II** (longer) and **III** (shorter), which differ from each other by less than 3%.



The global singlet minimum for X = H is shown in Figure 1a. One can imagine this structure as derived from structure **I** by removal of the PH<sub>3</sub> ligand *trans* to the H atom, whereas structure **III** may be imagined as derived by removal of a *cis*-PH<sub>3</sub> ligand. All X ligands used in this study, except for H, have a weaker *trans* influence than PH<sub>3</sub>, thus the Mo–PH<sub>3</sub> bond *trans* to X is stronger than the Mo–PH<sub>3</sub> bond *trans* to PH<sub>3</sub> except when X = H. A special word must be said about the methyl system, for which the “16-electron” global singlet minimum corresponds to a distorted geometry similar to **III** with an additional agostic interaction involving one of the methyl group H atoms (see Figure 1b). The agostic Mo···H distance in this optimized structure is 2.279 Å and the Mo–C–H angle is 82.7°. The agostic C–H bond is slightly longer (1.137 Å) than the other two C–H bonds (1.098 and 1.100 Å). The preference for this agostic structure agrees well with the C–H oxidative addition reactivity established for complexes CpMo(CH<sub>3</sub>)(PMe<sub>3</sub>)<sub>3</sub> and for the Cp\* analogue.<sup>55</sup> An estimate of the strength of this agostic interaction was obtained by imposing identical Mo–C–H angles for the Mo–CH<sub>3</sub> moiety during the optimization. This structure was found to be 3.7 kcal/mol less stable than that of Figure 1b.

Geometrical distortions similar to those observed here for singlet CpMoX(PH<sub>3</sub>)<sub>2</sub> have previously been analyzed computationally for related electronically unsaturated systems, for instance 16-electron d<sup>6</sup> and d<sup>4</sup> CpML<sub>n</sub> systems.<sup>25,56–58</sup> To

(46) Hay, P. J.; Wadt, W. R. *J. Chem. Phys.* **1985**, *82*, 299–310.

(47) Cacelli, I.; Keogh, D. W.; Poli, R.; Rizzo, A. *J. Phys. Chem. A* **1997**, *101*, 9801–9812.

(48) Poli, R.; Smith, K. M. *Eur. J. Inorg. Chem.* **1999**, 877–880.

(49) Poli, R.; Smith, K. M. *Eur. J. Inorg. Chem.* **1999**, 2343–2346.

(50) Siegbahn, P. E. M. *J. Am. Chem. Soc.* **1996**, *118*, 1487–1496.

(51) Wang, W.; Weitz, E. *J. Phys. Chem. A* **1997**, *101*, 2358–2363.

(52) Yang, H.; Asplund, M. C.; Kotz, K. T.; Wilkens, M. J.; Frei, H.; Harris, C. B. *J. Am. Chem. Soc.* **1998**, *120*, 10154–10165.

(53) Davidson, E. R.; Feller, D. *Chem. Rev.* **1986**, *86*, 681–696.

(54) Boys, S. F.; Bernardi, F. *Mol. Phys.* **1970**, *19*, 553–566.

(55) Abugideiri, F.; Kelland, M. A.; Poli, R.; Rheingold, A. L. *Organometallics* **1992**, *11*, 1303–1311.

(56) Kubáček, P.; Hoffmann, R.; Havlas, Z. *Organometallics* **1982**, *1*, 180–188.

(57) Ward, T. R.; Schafer, O.; Daul, C.; Hofmann, P. *Organometallics* **1997**, *16*, 3207–3215.

(58) Smith, K. M.; Poli, R.; Legzdins, P. *Chem. Commun.* **1998**, 1903–1904.



**Table 1.** Relevant Energetic Parameters for the  $\text{PH}_3$  Dissociation from  $\text{CpMoX}(\text{PH}_3)_3$  (see Schemes 1 and 2)<sup>a</sup>

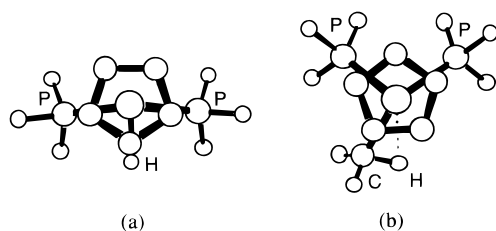
X	BDE (Mo–PH <sub>3</sub> ) (triplet)	BDE (Mo–PH <sub>3</sub> ) (singlet)	$\Delta E_{\text{S-T}}^b$	$\Delta E_{\pi}^c$ (singlet)	$\Delta E_{\pi}^c$ (triplet)	$\Delta E_{\text{steric}}^d$ (singlet)	$\Delta E_{\text{steric}}^e$ (triplet)
H	23.5	25.3	1.8	–2.0	1.3	1.0	–0.6
Me	13.2	16.3	3.1	7.0	11.7	1.0	0.3
F	6.3	14.9	8.7	7.7	19.3	1.7	–0.2
Cl	5.9	13.4	7.5	2.8	14.3	8.1	5.2
Br	6.5	13.6	7.0	1.8	13.1	9.0	5.7
I	9.1	15.7	6.6	4.2	15.3	4.5	1.0
OH	4.5	6.2	1.7	14.1	18.8	4.1	2.1
PH <sub>2</sub>	14.9	7.0	–7.9	16.0	10.2	1.3	0.3

<sup>a</sup> All energies are in kcal/mol. <sup>b</sup>  $\Delta E_{\text{S-T}} = E_{\text{singlet}} - E_{\text{triplet}}$ . <sup>c</sup>  $\Delta E_{\pi} = \text{BET}(\text{Mo-X } \sigma + \pi) - \text{BET}(\text{Mo-X } \sigma)$ . <sup>d</sup>  $\Delta E_{\text{steric}}(\text{singlet}) = -\Delta E_1 + \Delta E_2$ . <sup>e</sup>  $\Delta E_{\text{steric}}(\text{triplet}) = -\Delta E_1 + \Delta E_3$ .

**Table 2.** Selected Optimized Bond Angles (°) and Lengths (Å) for  $\text{CpMoX}(\text{PH}_3)_n$  ( $n = 3, 2$ )

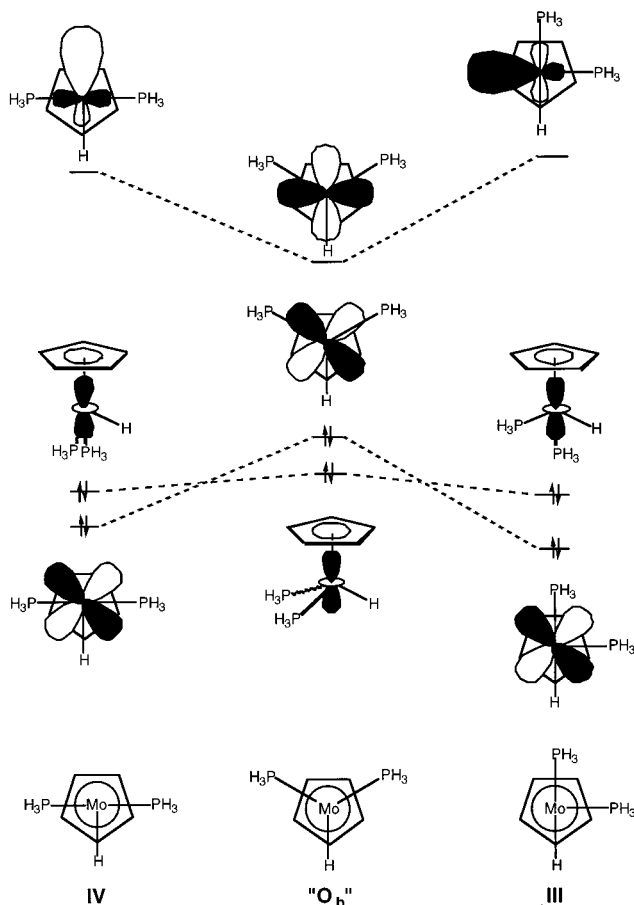
	X	H <sup>a</sup>	CH <sub>3</sub>	F	Cl	Br	I	OH	PH <sub>2</sub>
$n = 3$	Mo–X	1.722	2.299	2.085	2.633	2.805	3.002	2.095	2.696
$n = 2$	Mo–X	1.739	2.193	1.993	2.472	2.627	2.806	2.012	2.565
<b>II</b> (triplet)	$\xi(\text{Mo-X})^b$	–0.99	4.6	4.4	6.1	6.3	6.5	4.0	4.9
	$\theta^c$	0.0	0.1	0.0	0.0	0.0	0.0	0.0	6.7
	$\phi^c$	159.0	130.7	123.4	120.0	119.0	117.2	123.6	129.0
$n = 2$	Mo–X	1.723	2.126	1.994	2.463	2.611	2.781	1.972	2.326
<b>III</b> (singlet)	$\xi(\text{Mo-X})^b$	–0.06	7.5	4.4	6.5	6.9	7.4	5.9	13.7
	$\theta^c$	43.9	26.0	25.5	13.1	6.4	0.3	10.5	1.2
	$\phi^c$	105.7	102.0	102.2	102.4	102.3	101.9	102.7	102.6

<sup>a</sup> The lowest energy  $n = 2$  (singlet) structure (see Figure 1a) has Mo–H = 1.700 Å,  $\xi(\text{Mo-X}) = 1.2$ ,  $\theta = 1.4^\circ$  and  $\phi = 188.7^\circ$ . <sup>b</sup>  $\xi(\text{Mo-X}) = \{[\text{Mo-X} (n = 3) - \text{Mo-X} (n = 2)]/[\text{Mo-X} (n = 3)]\} \cdot 100$ . <sup>c</sup> See drawing **III**.

**Figure 1.** MacMoMo<sup>70</sup> view of the optimized structures of singlet  $\text{CpMoH}(\text{PH}_3)_2$  (a) and  $\text{CpMo}(\text{CH}_3)(\text{PH}_3)_2$  (b). The cyclopentadienyl H atoms are omitted for clarity.

explain the geometries observed for the singlet  $d^4$   $\text{CpMoX}(\text{PH}_3)_2$  systems, the Kohn and Sham orbitals of the highly distorted hydride species were examined in detail. The use of these orbitals for both qualitative and quantitative assessments of chemical phenomena is well established.<sup>59–61</sup> The energies and shapes of the frontier orbitals of singlet  $\text{CpMoH}(\text{PH}_3)_2$  in various geometries are represented pictorially in Figure 2. In addition to the distorted optimized geometries (the higher energy local minimum, labeled **III**, and the global minimum **IV**), the orbitals of the undistorted, pseudo-octahedral (electronically speaking, when considering the Cp as occupying three mutually adjacent coordination positions) species were obtained via a single-point calculation on an idealized three-legged piano stool geometry, labeled “**O<sub>n</sub>**” in Figure 2.

The “**O<sub>n</sub>**” geometry has  $\text{PH}_3$  ligands that lie partially along the lobes of the highest occupied molecular orbital (HOMO). In both optimized structures **III** and **IV**, the distortion moves the  $\text{PH}_3$  ligands onto the nodal planes of this orbital, thereby

**Figure 2.** Frontier orbital evolution upon distortion of singlet  $\text{CpMoH}(\text{PH}_3)_2$  from an idealized three-legged piano stool geometry.

lowering it in energy so that it becomes the second highest occupied molecular orbital (SHOMO). The other doubly occupied orbital, the HOMO for **III** and **IV** and the SHOMO for

- (59) Baerends, E. J.; Gritsenko, O. V.; Van Leeuwen, R. In *Chemical Application of Density-Functional Theory*; B. B. Laird, Ed.; American Chemical Society: Washington D. C., 1996; Vol. 629, p 42.
- (60) Baerends, E. J.; Gritsenko, O. V. *J. Phys. Chem.* **1997**, *101*, 5383–5403.
- (61) Stowasser, R.; Hoffmann, R. *J. Am. Chem. Soc.* **1999**, *121*, 1, 3414–3420.

“O<sub>h</sub>”, has a nodal surface along the Mo–PH<sub>3</sub> and Mo–H bonds in all three cases, and so it remains essentially constant in energy. The same geometry change that stabilizes one of the filled orbitals causes the PH<sub>3</sub> groups to move onto the lobes of the lowest unoccupied molecular orbital (LUMO), leading to the destabilization and rehybridization of this orbital in **III** and **IV**. This effect is accompanied by the stabilization of the corresponding metal–ligand bonding combination, which provides an additional, perhaps more important, stabilizing effect. The net result is that both distortions induce a significant stabilization of two filled orbitals and the increase of the HOMO–LUMO gap, thereby improving the relative stability of the spin-paired complexes.<sup>62</sup> This orbital splitting is not desirable for the triplet spin state and triplet CpMoH(PH<sub>3</sub>)<sub>2</sub> does not exhibit these deformations. Parallels may be drawn to the studies of Eisenstein and co-workers, who demonstrated that although triplet d<sup>6</sup> ML<sub>5</sub> compounds have undistorted trigonal bipyramidal structures,<sup>63</sup> two different deformation modes exist for the singlet species, the relative energy of which depend on the  $\pi$ - and  $\sigma$ -bonding properties of the ancillary ligands.<sup>64,65</sup>

Although the geometric distortions are most pronounced for X = H and Me (see Table 2), large effects are also displayed for the F, Cl, and OH singlet complexes and the distortions are progressively smaller for Br, PH<sub>2</sub>, and I systems. This variation with respect to the identity of the X ligand presumably is the result of competing  $\sigma$  and  $\pi$  effects. For the hydride and methyl, no significant  $\pi$  donation interactions are possible, and so geometric distortions are the only available option to decrease the total energy. For X =  $\pi$ -donor ligand, the orbital energies are also influenced by  $\pi$  donation,<sup>8,11</sup> which is equally effective in a nondistorted geometry. Thus, although F and OH have stronger  $\pi$ -donating properties (vide infra), they also provide a stronger  $\sigma$  component leading to significant distortions.

All optimized parameters compare rather well with those observed experimentally for available related systems. The calculations correctly reproduce the observed ground state for all those 16-electron systems that have been isolated or observed in solution: Cp\*Mo(PR<sub>2</sub>)(PMe<sub>3</sub>)<sub>2</sub> is diamagnetic,<sup>66</sup> whereas Cp\*MoCIL<sub>2</sub> (L = PMe<sub>3</sub>, PMe<sub>2</sub>Ph or L<sub>2</sub> = dppe)<sup>7,8</sup> and CpMo(OH)(PMe<sub>3</sub>)<sub>2</sub><sup>10,11</sup> have two unpaired electrons. The calculated Mo–PH<sub>3</sub> BDEs (Table 1) are also consistent with the observed relative stability of the various 18-electron systems; although no PMe<sub>3</sub> dissociation from CpMoH(PMe<sub>3</sub>)<sub>3</sub> occurs under ambient conditions,<sup>11</sup> the same dissociation from CpMo(CH<sub>3</sub>)(PMe<sub>3</sub>)<sub>3</sub> and Cp\*Mo(CH<sub>3</sub>)(PMe<sub>3</sub>)<sub>3</sub> readily takes place at 40 °C and room temperature, respectively, leading to metalation of the PMe<sub>3</sub> and Cp\* ligand, respectively.<sup>55</sup> In addition, Cp\*MoCl(PMe<sub>3</sub>)<sub>3</sub> establishes an observable equilibrium with Cp\*MoCl(PMe<sub>3</sub>)<sub>2</sub> and PMe<sub>3</sub>,<sup>8</sup> and finally CpMo(OH)(PMe<sub>3</sub>)<sub>3</sub> does not exist. Steric effects are certainly involved in further stabilizing the unsaturated structure with respect to the computed PH<sub>3</sub> model system (see below). In addition, the use of the PH<sub>3</sub> model usually leads to weaker Mo–P bonds relative to PMe<sub>3</sub>.<sup>67,68</sup>

(62) Kubáček, P.; Hoffmann, R. *J. Am. Chem. Soc.* **1981**, *103*, 4320–4332.

(63) Riehl, J.-F.; Jean, Y.; Eisenstein, O.; Pélissier, M. *Organometallics* **1992**, *11*, 729–737.

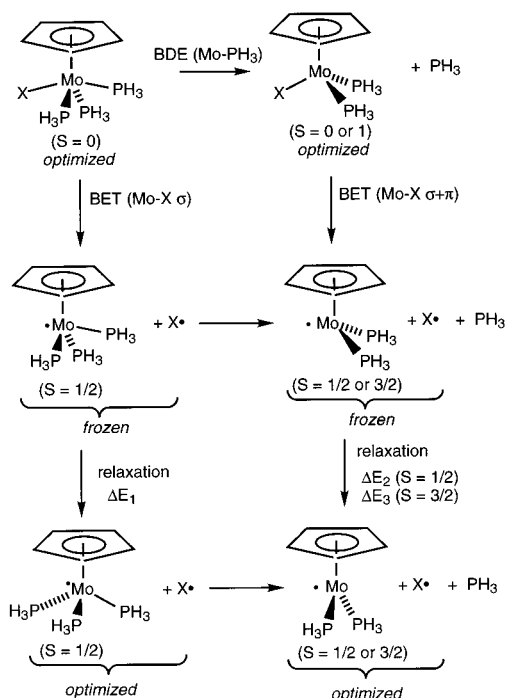
(64) El-Idrissi, I.; Eisenstein, O.; Jean, Y. *New J. Chem.* **1990**, *14*, 671–677.

(65) Albinati, A.; Bakmutov, V. I.; Caulton, K. G.; Clot, E.; Eckert, J.; Eisenstein, O.; Gusev, D. G.; Grushin, V. V.; Hauger, B. E.; Klooster, W. T.; Koetzle, T. F.; McMullan, R. K.; O’Laughlin, T. J.; Pélissier, M.; Ricci, J. S.; Sigalas, M. P.; Vymenits, A. B. *J. Am. Chem. Soc.* **1993**, *115*, 7300–7312.

(66) Baker, R. T.; Calabrese, J. C.; Harlow, R. L.; Williams, I. D. *Organometallics* **1993**, *12*, 830–841.

(67) Schmid, R.; Herrmann, W. A.; Frenking, G. *Organometallics* **1997**, *16*, 701–708.

Scheme 2



**b. Extent of the Mo–X  $\pi$  Stabilization.** As qualitatively discussed previously,<sup>7</sup> an X ligand with two lone pairs (double-sided  $\pi$  donor) should interact with a 16-electron metal fragment by establishing one two-center, two-electron  $\pi$  bond with the empty metal orbital in the singlet state and two two-center, three-electron  $\pi$  interactions with the two singly occupied metal orbitals in the triplet state. Thus, for both spin states, a double-sided  $\pi$  donor can transfer two  $\pi$  electrons overall to the metal center. In addition, a four-electron destabilizing interaction is present in both spin states. On the other hand, a single-sided  $\pi$  donor can donate both  $\pi$  electrons only in the singlet structure, whereas a one-electron  $\pi$  stabilization (one-half bond order) occurs for the triplet structure. Finally,  $\pi$ -neutral X ligands should establish only a pure  $\sigma$  interaction in both singlet and triplet 16-electron systems, as in the 18-electron system.

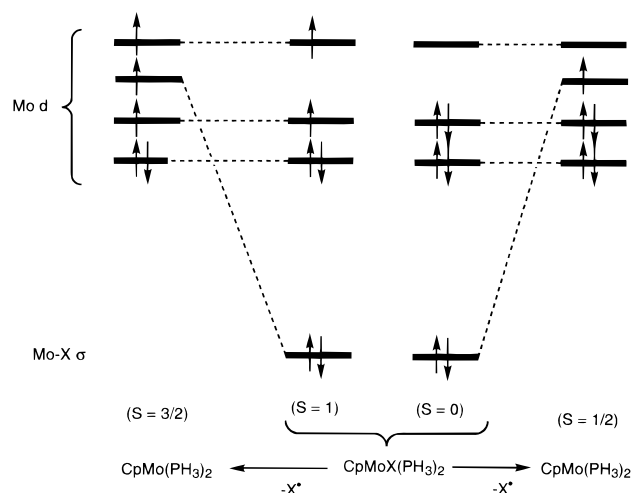
Breaking the Mo–X bond in **I** gives the radical pair CpMo(PH<sub>3</sub>)<sub>3</sub>• and X•, both in the doublet state (Scheme 2). Energies for these systems are calculated in the frozen geometry derived from optimized CpMoX(PH<sub>3</sub>)<sub>3</sub>, providing the so-called Bond Energy Terms (BET),<sup>69</sup> which are a measure of the Mo–X  $\sigma$ -bond strengths. The analogous process on **II** and **III** gives a BET that may be related to the strength of the ( $\sigma$  +  $\pi$ ) interaction. The subtraction of the Mo–X BET (18-electron system) from the Mo–X BET (16-electron system) gives us an evaluation of the stabilization provided to the unsaturated system by the establishment of the  $\pi$  interaction ( $\Delta E_\pi$ ). The results obtained are listed in Table 1. These values are essentially unaffected by the BSSE, as the individual BETs are affected by BSSE by essentially the same amount. For instance, a counterpoise correction for the fluoride system has given decreases in BET of 3.0, 2.6, and 2.6 kcal/mol for **I**, **II**, and **III**, respectively, leading to a correction of less than 0.5 kcal/mol for  $\Delta E_\pi$ .

The calculated  $\Delta E_\pi$  values for the triplet state are skewed by the influence of X on the electron-pairing energies. In fact,

(68) Gonz  lez-Blanco, O.; Branchadell, V. *Organometallics* **1997**, *16*, 5556–5562.

(69) Martinho Sim  es, J. A.; Beauchamp, J. L. *Chem. Rev.* **1990**, *90*, 629–688.

## Scheme 3



removal of  $\text{X}^\bullet$  from triplet  $\text{CpMoX}(\text{PH}_3)_2$  correlates with the spin quartet state, as shown in Scheme 3 (left). Therefore, there is a larger exchange interaction in this case relative to singlet system (Scheme 3, right). This is the reason for the much larger  $\Delta E_\pi$  values calculated for the triplet systems (Table 1). Even without pairing energy problems (i.e. for the singlet state), the deduction of a “ $\pi$ -bond strength” from the  $\Delta E_\pi$  values requires several approximations: (i) considering the  $\sigma$  bond as having the same strength in **I** and **III**; (ii) neglecting the rehybridization of X; (iii) neglecting the rehybridization of M; (iv) neglecting variations in the other M–L bonds. A  $\pi$  interaction compresses the Mo–X bond (lengths and shortening factors are shown in Table 2), weakening the  $\sigma$  component of the bond, although the bond becomes stronger overall. This approximation leads to an underestimation of  $\Delta E_\pi$ . Single-point calculations for **I** at the Mo–X distance of **III** show that this underestimation is 0.0 for H (as expected for a  $\pi$  neutral ligand) and up to 3.4 kcal/mol for the halides. The effect of the rehybridization of X is important only for  $\text{PH}_2$ , again leading to an underestimation of the  $\pi$ -bond strength for this ligand. The effect of a metal rehybridization is clearly illustrated by the structural distortions on going from **I** to **II** and **III**. The other Mo–ligand bonds do not appear to vary greatly, but how these small variations reflect into energy changes cannot be evaluated easily. In the absence of all these effects, the  $\Delta E_\pi$  value for the  $\pi$ -neutral H ligand should be exactly zero. The small negative value calculated for X = H (see Table 1) is an estimate of the limitations of these approximations. It should also be kept in mind that there is a nonzero (destabilizing)  $\pi$  interaction between the X and the metal lone pairs in  $\text{CpMoX}(\text{PH}_3)_3$ . The calculated  $\Delta E_\pi$  values actually reflect the combination of this filled-filled repulsion<sup>4</sup> at the 18-electron level and the  $\pi$  stabilization at the 16-electron level.

The  $\Delta E_\pi$  results in Table 1 lend themselves to several considerations. Although a Mo–X  $\pi$ -bond strength for the triplet state cannot be deduced from the data, the trend of the  $\Delta E_\pi$  values are approximately the same for the singlet and triplet species. In addition, although  $\Delta E_\pi$  (triplet) is greater than  $\Delta E_\pi$  (singlet) for all double-sided  $\pi$  donors, it is smaller for the phosphido ligand, confirming the qualitative considerations made above. This is probably the main reason for the adoption of a singlet ground state by the phosphido complexes. The action of the X ligands as  $\pi$  donors in the triplet complexes can also be judged by the percent of Mo–X bond shortening ( $\xi$ , see Table 2), which is similar for triplet and singlet complexes containing double-sided  $\pi$ -donor ligands (i.e. the halogens). The

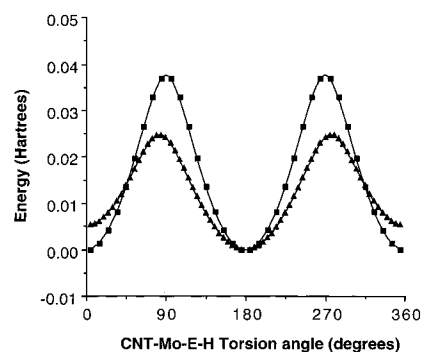


**Figure 3.** Plot of the energy of  $\text{CpMo}(\text{EH}_n)(\text{PH}_3)_2$  ( $S = 0$ ) vs the CNT-Mo–E–H dihedral angle. All other geometrical parameters are those of the optimized geometry. Squares: E = P,  $n = 2$ ; triangles: E = O,  $n = 1$ .

$\text{PH}_2$  ligand, being able to provide only one  $\pi$  electron in the triplet state, leads to a significant increase of  $\xi$  on going from triplet **II** to singlet **III**. The OH case is interesting,  $\xi$  increasing by 50% on going from triplet to singlet. Although the OH ligand acts as a double-sided  $\pi$  donor,<sup>11</sup> one orbital interaction is stronger than the other one leading to a weaker interaction in the triplet state. As a result,  $\xi(\text{F}) > \xi(\text{OH})$  for triplet **II**, whereas the reverse holds true for singlet **III**.

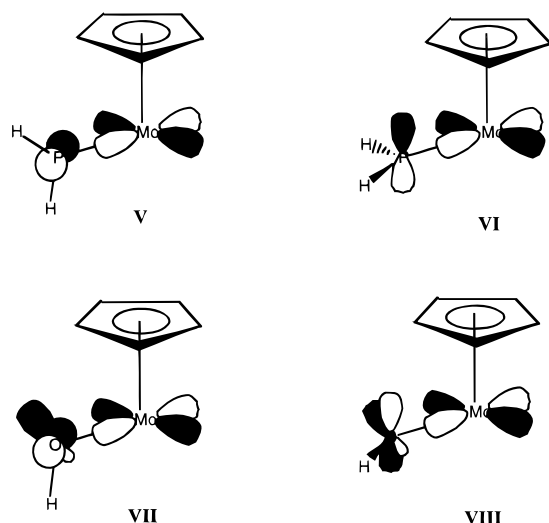
The  $\Delta E_\pi$  value calculated for F is significantly greater than zero, in agreement with the notion that the fluoride ion is a good  $\pi$ -donor ligand. The values calculated for the other halides are smaller but positive. Within the halogen group, however, the trend is not monotonic, iodide leading to a greater value than both chloride and bromide. Given the approximations alluded to above, we do not believe that too much emphasis should be placed on this trend. However, the results are in agreement with the halogens having a small but significant  $\pi$ -donating capability. The methyl ligand shows a 7.5% contraction for the agostic structure of Figure 1b. This shortening accompanies the high  $\Delta E_\pi$  value, which obviously is a measure of the strength of the Mo–CH<sub>3</sub> agostic interaction rather than a  $\pi$  interaction. Finally, the much larger values calculated for OH and  $\text{PH}_2$  agree well with the known strong  $\pi$ -donor power of hydroxide, alkoxides, aryloxides, and dialkyl- and diarylphosphido ligands.

Somewhat surprisingly, the percent of Mo–X bond shortening  $\xi(\text{Mo–X})$  in Table 2 does not correlate with the  $\Delta E_\pi$  values. The smallest change is seen, as expected, for the  $\pi$ -neutral H ligand. For the halogen series, the percent contraction increases in the order  $\text{F} < \text{Cl} < \text{Br} < \text{I}$  (in both spin states), whereas F has the greater  $\Delta E_\pi$  value. Also, OH has a  $\Delta E_\pi$  value similar to that of  $\text{PH}_2$  (for the singlet) but a much smaller  $\xi(\text{Mo–X})$  value, similar to those of the halogens. These data illustrate that the percent bond contraction should not be used in general as a measure of relative  $\pi$ -bond strengths.

An independent evaluation of the  $\pi$ -bond strength has been obtained for those ligands, namely OH and  $\text{PH}_2$ , for which the strength of the  $\pi$  interaction depends on the angular orientation. For singlet  $\text{CpMoX}(\text{PH}_3)_2$  (X = OH,  $\text{PH}_2$ ), single-point calculations have been performed on geometries derived from the optimized minimum by gradually rotating the X ligand around the Mo–X bond. The results are shown in Figure 3.

For the phosphido system, the maximum  $\pi$  overlap is achieved at the optimized geometry with CNT–Mo–P–H = 0° or 180°, whereas the orthogonal orientation gives a zero overlap (see **V** and **VI** in Scheme 4). The energy difference of 23.1 kcal/mol may be taken as an overestimation of the Mo– $\text{PH}_2$   $\pi$ -bond strength, because of the unrelaxed nature of the

Scheme 4



CpMo(PH<sub>3</sub>)<sub>2</sub> moiety in the rotated geometry. The window between this overestimated value and the underestimated one of Table 1 is relatively narrow.

For the hydroxide system, the two C<sub>s</sub>-symmetric structures (CNT–Mo–O–H angles of 0°, *endo*, see **VII**, and 180°, *exo*) are not identical, because of the greater filled-filled repulsion between the oxygen sp<sup>x</sup> lone pair and the Mo d<sub>z<sup>2</sup></sub> lone pair in the *exo* conformation. In the 90° conformation (**VIII**), Mo–O π bonding is not quite zero, because OH is still able to overlap with the Mo d<sub>xy</sub> orbital (albeit not as effectively) by using the sp<sup>x</sup> lone pair. At any rate, the energy difference between the most stable *exo* structure and the 90° maximum is 18 kcal/mol and is again slightly higher than the Δ*E*<sub>π</sub> values calculated for OH in Table 1.

**c. Steric Interactions.** The bond dissociation energy of PH<sub>3</sub> from CpMoX(PH<sub>3</sub>)<sub>3</sub> is modulated by π donation and by the release of pairing energy upon adoption of the triplet configuration, both being functions of the nature of X. However, differences in size and electronic environment for the various X ligands will also cause differences in the steric pressures exerted on the rest of the coordination sphere and provide an additional contribution to affect the Mo–PH<sub>3</sub> bond dissociation energy. These differences may be evaluated by comparing the relaxation energies of the fragments that are obtained from the Mo–X bond-breaking process for each system. Thus, (–Δ*E*<sub>1</sub> + Δ*E*<sub>2</sub>) = Δ*E*<sub>steric</sub> (singlet) is a measure of the release of steric pressure associated with the formation of the singlet 16-electron product, whereas (–Δ*E*<sub>1</sub> + Δ*E*<sub>3</sub>) = Δ*E*<sub>steric</sub> (triplet) measures the same parameter for the formation of the triplet product. These values are reported in Table 1. Positive values indicate greater pressure on the more saturated system, as expected. In some cases small values are obtained by subtraction of individual large relaxation energies. For each X ligand, the singlet state gives rise to a greater Δ*E*<sub>steric</sub> value. This result correlates with the greater distortion that the CpMo(PH<sub>3</sub>)<sub>2</sub> fragment has to withstand to lead to the triplet geometry upon binding X, thus more efficiently balancing out the greater relaxation experienced by the more saturated system.

We can immediately observe that the smallest X ligand, H, gives small steric contributions. The optimized geometries of both CpMo(PH<sub>3</sub>)<sub>3</sub> and CpMo(PH<sub>3</sub>)<sub>2</sub> fragments are quite close to those of the same fragments in the corresponding optimized hydrides, and the individual relaxation energies Δ*E*<sub>1</sub>, Δ*E*<sub>2</sub>, and Δ*E*<sub>3</sub> (3.2, 2.0, and 1.4 kcal/mol, respectively) are smaller than

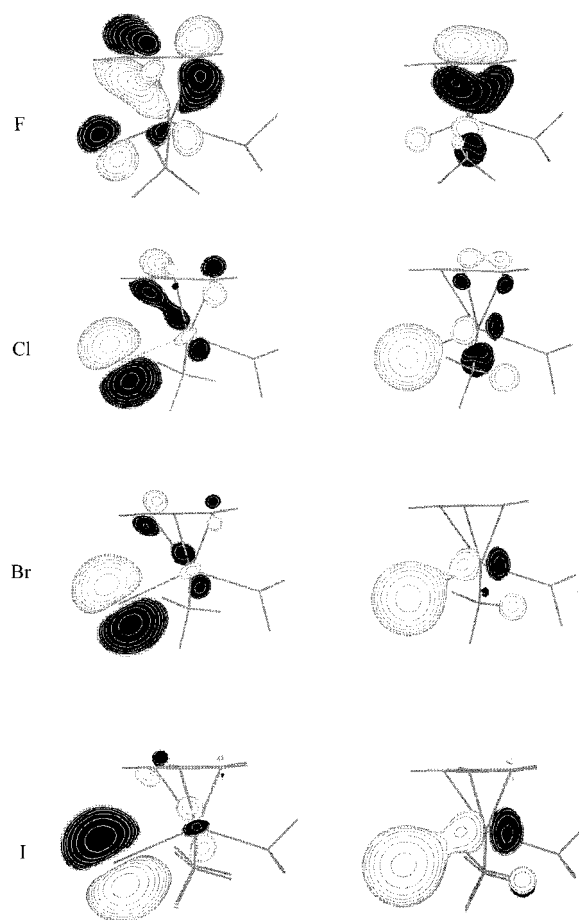


**Figure 4.** MOLDEN views of the third (left) and fourth (right) highest MO for CpMoX(PH<sub>3</sub>)<sub>3</sub>. The orbital contour lines correspond to 4% of the maximum electron density.

those of the other X ligands, indicating that H has a small steric influence in both 18-electron and 16-electron structures. It is notable that Δ*E*<sub>steric</sub> is relatively large for Cl and Br, whereas it is smaller for I and F. It is unexpectedly small for PH<sub>2</sub>, especially considering that the size of P is similar to that of Cl, and it is even smaller for CH<sub>3</sub>. These values suggest to us that the major steric repulsion derives from the interaction between the X lone pairs and the neighboring PH<sub>3</sub> ligands. The Cl and Br atoms have two *p* lone pairs oriented perpendicularly to the Mo–X bond, extending in the region of space occupied by the PH<sub>3</sub> ligands in the 18-electron complex (see Figure 4). On an energy scale, these two orbitals are placed immediately underneath the two filled metal orbitals. Correspondingly, OH has only one *p* lone pair (the second lone pair is a hybrid orbital pointing away from the PH<sub>3</sub> ligands,<sup>11</sup> as shown in **VII**), whereas PH<sub>2</sub> and CH<sub>3</sub> have none (the only P lone pair is a hybrid orbital with a large amount of *s* character, pointing away from the adjacent PH<sub>3</sub> ligands). This is a manifestation of an interligand *filled-filled* repulsion. The *filled-filled* repulsion between the X lone pairs and the filled metal orbitals, on the other hand, is accounted for in the Δ*E*<sub>π</sub> term.

It is interesting to observe the trend of Δ*E*<sub>steric</sub> values for the halogen series in the order (for both spin states) F < Cl ~ Br > I. This result is determined for the most part by the trend in the rearrangement factor Δ*E*<sub>1</sub> for the 18-electron compounds (7.11, 12.74, 13.35, and 8.7 kcal/mol for F, Cl, Br, and I, respectively). The small value of Δ*E*<sub>steric</sub> observed for F may be attributed to the small size of the atom and of its orbitals, leading to a small interaction with the adjacent PH<sub>3</sub> ligands.



The smaller value for I relative to Cl and Br, on the other hand, may be attributed to the longer distance and greater diffuseness of the orbitals. These considerations appear consistent with the shape of the orbitals as shown in Figure 4.

**d. Comparison of Stabilizing Effects.** In the three preceding sections, we examined the effects of the singlet–triplet conversion, of the  $\pi$  stabilization, and of the release of steric pressure to the relative stabilization of the open-shell system deriving from dissociation of a  $\text{PH}_3$  ligand from  $\text{CpMoX}(\text{PH}_3)_3$  (Schemes 1 and 2). The correction of the  $\text{Mo–PH}_3$  BDE (for either the singlet or the triplet 16-electron product) by the  $\Delta E_\pi$  and the  $\Delta E_{\text{steric}}$  parameters (Table 1) provides the BDE for the  $\text{Mo–PH}_3$  bond in geometry-optimized spin-doublet  $\text{CpMo}(\text{PH}_3)_3$  (relative to optimized doublet and quartet  $\text{CpMo}(\text{PH}_3)_2$ , respectively). These values are independent of the nature of X and are calculated as 24.3 and 25.4 kcal/mol, respectively, see eqs 1 and 2.

$$\text{BDE (singlet)} + \Delta E_\pi (\text{singlet}) + \Delta E_{\text{steric}} (\text{singlet}) = 24.3 \text{ kcal/mol} \quad (1)$$

$$\text{BDE (triplet)} + \Delta E_\pi (\text{triplet}) + \Delta E_{\text{steric}} (\text{triplet}) = 25.4 \text{ kcal/mol} \quad (2)$$

These values are very close to each other because the optimized doublet and quartet  $\text{CpMo}(\text{PH}_3)_2$  species have very similar energies and can be taken as measures of the “intrinsic”  $\text{Mo–PH}_3$  bond strength (for each spin state) in the absence of any stabilizing factor introduced by the presence of X. The introduction of X modulates these BDEs by stabilizing the less saturated and/or by destabilizing the more saturated structure by steric and  $\pi$ -bonding effects. The introduction of X also has a large effect on the electron-pairing energy, as shown by the variable singlet–triplet gap (varying from 8.7 kcal/mol for F to  $-7.9$  kcal/mol for  $\text{PH}_2$ ) for the 16-electron  $\text{CpMoX}(\text{PH}_3)_2$ , compared with the doublet–quartet gap of  $-1.10$  kcal/mol for the 15-electron  $\text{CpMo}(\text{PH}_3)_2$ .

It is impossible to completely separate the effects caused by these stabilizing factors when one wishes to analyze the stabilization of *triplet*  $\text{CpMoX}(\text{PH}_3)_2$  (i.e. the ground state in all cases except for  $\text{X} = \text{PH}_2$ ) and free  $\text{PH}_3$  relative to *singlet*  $\text{CpMoX}(\text{PH}_3)_3$ , because these effects are linked to the structural changes associated with the change of spin state. We have already pointed out that pairing energy effects and  $\pi$ -bonding effects are combined in the  $\Delta E_\pi$  term in eq 2. A convenient, although admittedly limited, approach is given in eq 3.

$$\text{BDE (triplet)} + \Delta E_{\text{S–T}} + \Delta E_\pi (\text{singlet}) + \Delta E_{\text{steric}} (\text{singlet}) = 24.3 \text{ kcal/mol} \quad (3)$$

This approach corresponds to the following stepwise process. The optimized  $\text{CpMo}(\text{PH}_3)_3$  on one side and the combination of optimized *doublet*  $\text{CpMo}(\text{PH}_3)_2$  and free  $\text{PH}_3$  on the other side (relative energy, 24.3 kcal/mol) are distorted to the geometries of the corresponding fragments in the adducts with X [ $\Delta E_{\text{steric}}$  (singlet)]. Subsequently,  $\text{X}^\bullet$  is added to form the  $\text{Mo–X}$  bond, involving BET ( $\sigma$ ) for  $\text{CpMoX}(\text{PH}_3)_3$  and BET ( $\sigma + \pi$ ) for  $\text{CpMoX}(\text{PH}_3)_2$  [ $\Delta E_\pi$  (singlet)]. Finally, singlet  $\text{CpMoX}(\text{PH}_3)_2$  is relaxed to the triplet ground state ( $\Delta E_{\text{S–T}}$ ). Although this scheme has limitations because of the interrelated nature of these effects, the same would hold true for possible alternative schemes.

The comparison of the  $\Delta E_{\text{S–T}}$ , singlet  $\Delta E_\pi$ , and singlet  $\Delta E_{\text{steric}}$  values in Table 1 for each X give interesting indications on the relative importance of spin-pairing effects, ligand  $\pi$  donation, and release of steric pressure for the relative stabilization of the 16-electron  $\text{CpMoX}(\text{PH}_3)_2$  and therefore for the dependence of the  $\text{Mo–PH}_3$  bond dissociation energy on the nature of X. The hydride system has a relatively unencumbering ( $\Delta E_{\text{steric}} = 1.0$  kcal/mol) and  $\pi$ -neutral ( $\Delta E_\pi = -2.0$  kcal/mol) X group. Because the triplet state is only slightly stabilized relative to the singlet one ( $\Delta E_{\text{S–T}} = 1.8$  kcal/mol), the  $\text{Mo–PH}_3$  BDE is quite close to the “intrinsic” bond strength found in  $\text{CpMo}(\text{PH}_3)_3$  and is the highest found for the series of X systems investigated in this study. For all other X systems, the  $\text{Mo–PH}_3$  BDE drops dramatically, but for different reasons. As discussed earlier, the steric stabilization is mostly related to the presence of inactive lone pairs. For the  $\pi$  neutral  $\text{CH}_3$  system, there is essentially no sterics-related stabilization, whereas a significant  $\Delta E_\pi$  stabilization is related to the establishment of an agostic  $\text{Mo–C–H}$  interaction. The change of spin state also contributes to a large extent to the stabilization of the 16-electron methyl system. We cannot rationalize the difference between  $\Delta E_{\text{S–T}}$  for H and  $\text{CH}_3$ . The halogen systems are stabilized to a significant extent by each of the three effects, the  $\Delta E_{\text{S–T}}$  stabilization being nearly the same for all four (in the 8.7–6.6 kcal/mol interval, predictably in the order  $\text{F} > \text{Cl} > \text{Br} > \text{I}$ ), whereas the other two effects vary as a function of X in a way to provide an approximately identical total contribution (in the 9–11 kcal/mol range; mostly  $\Delta E_\pi$  for F, mostly  $\Delta E_{\text{steric}}$  for Cl and Br, and about 50:50 for I). The OH system experiences an even greater overall stabilization, which is mostly due to O–M  $\pi$  donation, but  $\Delta E_{\text{S–T}}$  and  $\Delta E_{\text{steric}}$  also play a role, especially the  $\Delta E_{\text{steric}}$ . Finally, the  $\text{PH}_2$  system (which is the only one examined here to adopt a singlet ground state) is stabilized almost entirely by  $\pi$  effects, whereas the steric factor is nearly zero.

## Conclusions

We have examined the relative importance of three difference factors (pairing energy associated to a spin-state change,  $\pi$  donation from ligand lone pairs, and release of steric pressure) in the relative stabilization of the  $\text{PH}_3$  dissociation product from  $\text{CpMoX}(\text{PH}_3)_3$  as a function of X ( $\text{X} = \text{H}, \text{CH}_3, \text{F}, \text{Cl}, \text{Br}, \text{I}, \text{OH},$  and  $\text{PH}_2$ ). These are model systems for a class of phosphine-substituted half-sandwich Mo(II) compounds, which exhibit richness in structure, magnetic properties, and chemical reactivity. This study has shown that the three effects can display all possible orders of relative importance depending on the nature of the donor atom, on the presence of inactive lone pairs, and on the number of  $\pi$  orbitals available ( $\pi$  neutral, single- or double-sided  $\pi$  donor). The spin-state change plays a dominant role for the stabilization of the halide derivatives and the methyl derivative. The study has further shown a contribution to stabilization from the  $\text{CH}_3$  group attributable to the establishment of an  $\alpha$ -agostic interaction.

**Acknowledgment.** We are grateful to the Conseil Régional de Bourgogne for support and to the European Commission for a Marie Curie postdoctoral fellowship to K.M.S. We also thank Odile Eisenstein for helpful discussion.

IC990875I

(70) Dobler, M. *Laboratory for Organic Chemistry*; ETH: Zürich, Switzerland, 1996.